Can Early Dark Energy be Detected in Non-Linear Structure?[*]

Matthew J. Francis[1][*], Geraint F. Lewis[1] and Eric V. Linder[2]

[1] *School of Physics, University of Sydney, NSW 2006, Australia*
[2] *University of California, Berkeley Lab, Berkeley, CA 94720, USA*

ABSTRACT

We present the first study of early dark energy cosmologies using N-body simulations to investigate the formation of non-linear structure. In contrast to expectations from semi-analytic approaches, we find that early dark energy does not imprint a unique signature on the statistics of non-linear structures. Investigating the non-linear power spectra and halo mass functions, we show that universal mass functions hold for early dark energy, making its presence difficult to distinguish from ΛCDM. Since early dark energy biases the baryon acoustic oscillation scale, the lack of discriminating power is problematic.

Key words: methods:N-body simulations — methods: numerical — dark matter — dark energy — large-scale structure of Universe

1 INTRODUCTION

Uncovering the nature of the dominant energy component of the Universe at the current epoch, dark energy, is a central goal of modern precision cosmology. The evidence for the existence of dark energy is strong (Riess et al. (1998), Perlmutter et al. (1999), Komatsu et al. (2008)), however on the theoretical front there are no leading candidates despite a wealth of suggestions (see Copeland, Sami & Tsujikawa (2006) for a review). As observational data becomes more precise and extensive due to current and future generations of large surveys and increasingly powerful instruments, there remains a number of theoretical challenges to determine with high accuracy the expected observational consequences of the myriad of possible dark energy models.

Dark energy affects the Universe primarily through the global expansion rate. This can be measured directly through distance measurements such as from Type Ia supernovae (Riess et al. (1998), Perlmutter et al. (1999), Kowalski et al. (2008)) over the last 10 billion years. However, some dark energy models predict a non-negligible contribution to the early time expansion behavior, called early dark energy (EDE). To probe EDE requires observations tied to the very high redshift universe, such as the cosmic microwave background (CMB) or baryon acoustic oscillations (BAO). However, as shown in Linder & Robbers

(2008), early dark energy can be hidden in CMB observations, even while shifting the intrinsic acoustic scale upon which BAO measurements rely upon. Thus failure to detect EDE can bias the cosmological model interpreted from CMB and BAO data.

An alternative and complementary measure of dark energy is through the observation of structure in the Universe. The change in the dynamical evolution of expansion relative to the ΛCDM model, say, alters the growth of structures in the inhomogeneous universe that we inhabit. The statistics of structure therefore encodes information about dark energy. Structure measures involve a different weighting of cosmological parameters than distance measures, thus the combination breaks degeneracies. Moreover, they can test the framework of gravitational growth of inhomogeneities, important for distinguishing between a physical dark energy and changes to the laws of gravity. Finally, growth is a cumulative process, depending on the physical conditions from early times through the epoch at which the structure is observed. Thus, observations of structure are crucial to understanding cosmology at all epochs. Because of the implications of early dark energy for interpreting CMB and BAO measurements, and for understanding the fundamental physics behind dark energy, the behavior of structure formation and evolution is a key point.

Early dark energy models address the coincidence problem by having the dark energy evolve relatively slowly compared to the dominant matter or radiation component; in some cases motivated by string theory they scale exactly with the background component. Indeed, this was one of the first dark energy models (Wetterich 1988). EDE is discussed in some detail in Doran & Robbers (2006) and ref-

erences therein. Constraints from CMB and primordial nucleosynthesis data restrict the energy fraction in the early universe contributed by EDE to less than a few percent (Doran, Robbers & Wetterich 2007) but this could have significant effects. Some of the implications for linear growth were examined in Linder (2006) and Doran & Robbers (2006) and extended semi-analytically to non-linear theory by Bartelmann, Doran & Wetterich (2006). The main result of previous studies of the non-linear growth in EDE cosmologies (such as Bartelmann, Doran & Wetterich (2006) and Fedeli & Bartelmann (2007)) is that for a fixed linear theory matter perturbation amplitude at $z = 0$, σ_8, there are more collapsed structure in EDE models than ΛCDM. For higher redshifts this effect increases, for instance Bartelmann, Doran & Wetterich (2006) found that at $z = 1$, there are up to an order of magnitude more dark matter halos for higher halo masses ($M_{halo} \gtrsim 10^{15} M_\odot$). This can be simply interpreted as early dark energy, which does not appreciably cluster, suppressing the growth of structure at early times. Hence, to achieve the observed level of current structure, the early amplitude of clustering must have been greater. Other applications include the high Sunyaev-Zel'dovich amplitude possibly seen at high multipoles in the CMB (Sadeh et al. 2007; Waizmann & Bartelmann 2008) and the early formation of the first stars (Sadeh & Rephaeli 2008).

A key aim of this paper is to use N-body simulations to calculate the predicted number of dark matter halos in EDE cosmologies compared with ΛCDM. In particular, the non-linear level of structure is affected by the early growth in a way that can change predictions based on the usual linear growth factor at a particular epoch. We examine both the halo mass function giving the abundance of collapsed objects and the non-linear matter power spectrum. N-body simulations are a robust method of determining these statistics and this paper critically examines predictions previously made analytically.

In Section 2 we describe the N-body simulations we used to probe the effects of EDE on non-linear structure formation. We present the results for the abundance of dark matter halos in Section 3 and the results for the non-linear matter power spectrum in Section 4. We discuss the implication of our results and make concluding remarks in Section 5.

2   SIMULATION DETAILS

The simulations were performed using the cosmological N-body code GADGET2 (Springel 2005) suitably modified in order to model the expansion history for arbitrary dark energy models. The initial CDM power spectrum was determined using the CMB code CMBEASY (Doran 2005). Initial realisations of the density field were created using part of the COSMICS code (Ma & Bertschinger 1995), modified to allow an arbitrary initial power spectrum. Given the real space displacement field, $\Psi_0(\mathbf{x})$, generated from the linear power spectrum $P(k)$ at redshift zero, the initial grid of particles are perturbed using the Zel'dovich approximation (Zel'dovich 1970) resulting in the positions and velocities at the starting scale factor a_i of

$$\mathbf{x} = \mathbf{q} + \frac{D(a_i)}{D(1)}\Psi_0(\mathbf{q}) \tag{1}$$

$$\dot{\mathbf{x}} = \frac{\dot{D}(a_i)}{D(1)}\Psi_0(\mathbf{q}) \tag{2}$$

where $\mathbf{q}$ are the real space grid co-ordinates and $D(a)$ is the linear growth factor. The dots refer to derivatives with respect to cosmic time t. The linear growth factor and its derivative were calculated by numerically integrating the growth equation detailed in Linder & Jenkins (2003). In all cases, the starting redshift was kept consistent between the different physical models. In general the linear power spectrum shape varies in the different models compared and therefore we made initial conditions separately for each model, always ensuring that the initial fluctuation amplitude returned the desired σ_8 at $z = 0$. The power spectra measured from simulation outputs were compared to linear theory to ensure that the large scale power evolved as expected. All simulations and numerical analysis were performed on 'The Green Machine' supercomputer located at the Centre for Astrophysics and Supercomputing, Swinburne University.

The early dark energy model is parametrised through its dimensionless energy density as a function of redshift by (Doran & Robbers 2006)

$$\Omega_d(a) = \frac{\Omega_d^0 - \Omega_e(1 - a^{-3w_0})}{\Omega_d^0 + \Omega_m^0 a^{3w_0}} + \Omega_e(1 - a^{-3w_0}) \tag{3}$$

in which Ω_m^0 and Ω_d^0 are the density parameters of matter and dark energy today ($\Omega_m^0 = 1 - \Omega_d^0$ in a flat universe as assumed here), w_0 is the equation of state of dark energy today and Ω_e is the energy density fraction of dark energy at early times, $a \ll 1$. Note that our Ω_e corresponds to Ω_d^e from Doran & Robbers (2006). Strictly for the initial comparison to Bartelmann, Doran & Wetterich (2006), we also use the bending model of Wetterich (2004), defined as

$$\ln \frac{\Omega_d(a)}{\Omega_m(a)} = \ln \frac{\Omega_d^0}{\Omega_m^0} - \frac{3w_0 \ln a}{1 - b \ln a}. \tag{4}$$

In both cases the dark energy equation of state is given by the standard formula $w(a) = -(1/[3\Omega_d(1 - \Omega_d)])d\Omega_d/d\ln a$. Note that Doran, Robbers & Wetterich (2007) find that the marginal distributions of the likelihood for cosmological parameters other than dark energy are insensitive to the specific parametrisation.

In all the simulations using the EDE form of Eq. 3 the cosmological model used was a flat universe with: $\Omega_m = 0.3$, $\Omega_b = 0.048$, $h = 0.69$, $n = 0.98$, $\sigma_8 = 0.76$, and $w_0 = -1$, except where specified otherwise.

Dark matter halos in our simulation outputs were determined using two different methods. The first is the Friends of Friends (FOF) method (Davis et al. 1985) using a constant linking length parameter of $b = 0.2$. An alternative approach to defining halos in simulation outputs is the spherical overdensity method (SO) (see Lukić et al. (2008) for a detailed comparison of FOF and SO halo methods). To find the SO defined halos, we employed the MPI version of the

AMIGA Halo Finder [1] (AHF), successor of MHF introduced by Gill et al. (2004). In order to use this for EDE cosmologies, we made the appropriate modifications to the virial overdensity calculation.

The matter power spectrum was calculated utilising the 'chaining the power' method, as described in Smith et al. (2003), using the cloud in a cell grid assignment scheme.

The bulk of the simulations used 256^3 particles in a 256 Mpc/h box starting at redshift $z = 24$. For each model we performed eight simulations using different realisations of the initial density field. The power spectrum and halo mass functions were averaged over all realisations. Additional simulations were performed halving and doubling the box size as well as altering the starting redshift, softening length and accuracy parameters to ensure convergence. We also check that for Ω_e approaching zero, the power spectrum and halo results converged to the results for constant $w = w_0$ as expected. The results of these tests indicated that the power spectrum ratio results are at most $\sim 1\%$ altered by different numerical parameters, with the most important factor being box size which affected the power spectrum ratios mainly at high k. Starting redshift and softening length make little difference to the ratios. The halo mass function results were somewhat affected by changing box size, our results agreed with the analysis of Power & Knebe (2006) for the effect of box size on the mass function. The ratio results fluctuated at the level of $\sim 10\%$ with varying box size. We do not claim state of the art precision in our mass function results, however they are sufficiently accurate and converged to support our main thesis, as detailed in Section 3.

3 HALO MASS FUNCTION

The halo mass function (hereafter HMF), defined simply as the number of halos of a given mass expected per unit volume, $n(M, z)$, is an important theoretical and observational statistic of the dark matter density field. Indeed, the abundance is often claimed to be exponentially sensitive to the cosmology. The pioneering work of Press & Schechter (1974) related the expected mass function to the variance, $\sigma(R)$ on some length scale R of the linearly evolved density field and the linear collapse parameter, δ_c, which is derived from spherical collapse arguments and for ΛCDM is only a weak function of cosmology and redshift.

The advent of larger N-body simulations allowed this mass function to be tested rigorously, resulting in improvements that modified the basic functional form to include ellipsoidal collapse with parameters fit to simulation by Sheth & Tormen (1999). This in turn was improved upon by Jenkins et al. (2001) and more recently by Warren et al. (2006) with an alternative approach of fitting directly the multiplicity function

$$f(\sigma) = \frac{M}{\rho} \frac{dn}{d\ln\sigma^{-1}} \qquad (5)$$

by some function of σ without reference to the collapse parameter. Here ρ is the background matter density. In both

Jenkins et al. (2001) and Warren et al. (2006) universal formulas for the multiplicity function, valid for a range of cosmologies, were found. The effect of cosmology enters through the variance σ as a function of scale and redshift and the mean matter density. Writing the Press-Schechter style mass functions in this form gives results that are broadly in agreement with the Jenkins and Warren formulas with the latter being more accurate fits to numerical data, but qualitatively similar. Despite being formulated from ΛCDM, matter dominated and open cosmologies only, the Jenkins formula has been shown to be valid also for a large N-body simulation of a dynamical dark energy cosmology (Linder & Jenkins 2003).

In previous work on EDE cosmologies relying on estimation of the HMF, (such as Bartelmann, Doran & Wetterich (2006) and Fedeli & Bartelmann (2007)) the Sheth-Tormen mass function has been used to predict the relative halo abundance of EDE and ΛCDM cosmologies. This required determination of the linear collapse parameter for EDE cosmologies, for the derivation see Bartelmann, Doran & Wetterich (2006). The analysis using this mass function suggested a significant increase in the number of massive halos in EDE models compared to ΛCDM models with the same σ_8 today. This was particularly true at $z = 1$. However, it is not clear that the Press-Schechter style mass functions, relying on the collapse parameter, is to be preferred for these cosmologies over the universal mass function approach of Jenkins and of Warren. For ΛCDM, the difference between the approaches is solely the degree of accuracy across a range of halo masses, but the functions broadly agree.

However, in this work we compare the two approaches for EDE and find a marked qualitative difference in non-linear structure predictions, although they both use the same linear density behavior. We have reproduced Fig. 5 of Bartelmann, Doran & Wetterich (2006) which showed the ratio of the HMF to the ΛCDM case for two EDE models (both using the bending parametrisation of Wetterich (2004), see our Eq. 4), at $z = 0$ and $z = 1$. However, in our reproduction (see Fig. 1) we have also included the prediction using instead the Jenkins and Warren formulas (note that these curves overlap and can barely be distinguished on the scale shown). The Sheth-Tormen mass functions shown utilised the method for calculating the linear density contrast at collapse time, δ_c, for EDE cosmologies from Bartelmann, Doran & Wetterich (2006), which results in a quite different value from ΛCDM. As can be seen, the predictions of the Sheth-Tormen and the Jenkins-Warren approaches are very different, and it is not clear *a priori* which approach should be used in the absence of rigorous calculation via N-body simulations. In this work, we fill the gap in the literature by performing these simulations and halo analyses. Note that the difference in the halo abundance ratios predicted by the Jenkins and Warren formulas is negligible for all cosmologies studied in this work and in subsequent figures we plot a single line that represents the prediction of both of these approaches.

3.1 Press-Schechter vs. Jenkins-Warren

As a direct comparison to the work of Bartelmann, Doran & Wetterich (2006), we perform

---

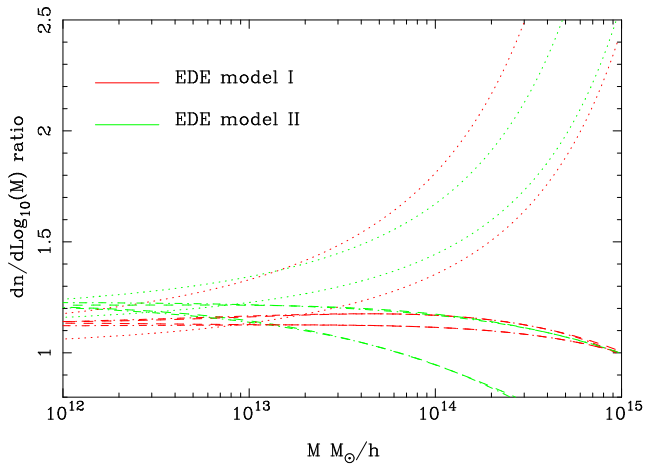[1] AMIGA is freely available for download at http://www.aip.de/People/AKnebe/AMIGA/

Figure 1. Reproduction of Fig. 5 of Bartelmann, Doran & Wetterich (2006) with the Jenkins et al. (2001) and Warren et al. (2006) mass functions also included. The Jenkins and Warren formulas are shown with dashed and dot-dashed lines respectively, however they are indistinguishable on this scale. They both clearly disagree with the Sheth-Tormen prediction, shown with dotted lines, for both models. For the Sheth-Tormen mass function, the upper curves are for $z = 1$ and the lower $z = 0$, however for the Jenkins-Warren mass functions the reverse is the case, the lower curves are for $z = 1$.

Figure 2. Mass function ratios at $z = 1$ between EDE and ΛCDM for different methods of predicting the mass function. The solid lines show the simulation data with halos found with the FOF method. The dot-dashed lines show the SO method results for the same data. The dashed lines show the Jenkins mass function (which gives almost the same prediction as the Warren formula). Finally, the dotted lines show the prediction of the Sheth-Tormen mass function. The Jenkins-Warren formula is clearly preferred by the simulation data.

simulations of the same two EDE and one ΛCDM models they considered analytically. Model I has $\Omega_{m,0}h^2 = 0.146$, $\Omega_b h^2 = 0.026$, $h = 0.67$, $n = 1.05$, $w_0 = -0.93$ and $\sigma_8 = 0.82$; Model II has $\Omega_{m,0}h^2 = 0.140$, $\Omega_b h^2 = 0.023$, $h = 0.62$, $n = 0.99$, $w_0 = -0.99$, and $\sigma_8 = 0.78$. Both models have an averaged value for the dark energy density during the matter dominated era of $\Omega_{d,sf} = 0.04$ (see Doran et al. (2001) for the precise definition).

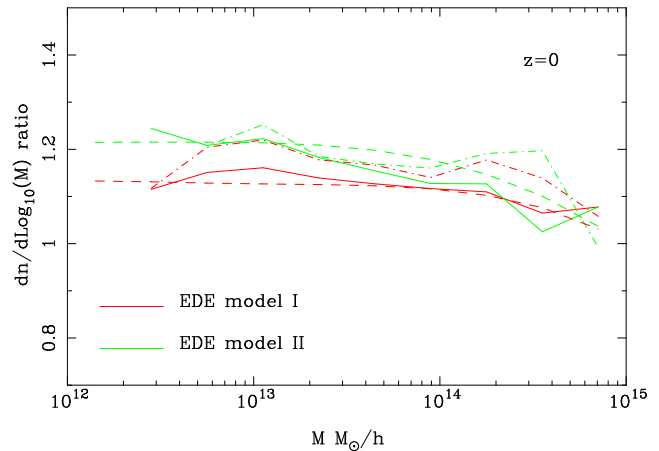The simulation results for the mass function, over-

Figure 3. Mass function ratios at $z = 0$ for the models described in Section 3.1. The line styles are the same as Fig. 2.

laid with the predictions from both the Sheth-Tormen and Jenkins-Warren mass functions, are shown in Figs. 2 and 3. The simulations show a good agreement with the predictions of the Jenkins formula and strong disagreement with the Sheth-Tormen function with the appropriate EDE linear collapse parameter. This has two crucial implications. The difference between ΛCDM and EDE in numbers of collapsed objects is much less than previously thought. Secondly, the abundance increase reverses at higher redshift, i.e. rather than an order of magnitude *more* halos in EDE at $z = 1$ as previously predicted, we find *less* halos at the high mass end for one of the models, and comparable number of halos at the low mass end.

This result is important and troubling; instead of the number of halos being exponentially sensitive and a crucial tool for detecting EDE, it appears that it is quite insensitive to the existence of EDE at the few percent energy density level, at or below the upper limit satisfying current data. The implications are further discussed in Section 5.

3.2 Early Dark Energy Mass Functions

Although we used the bending model of EDE for direct comparison to Bartelmann, Doran & Wetterich (2006), an improved model of EDE was formulated after that paper. We treat the EDE model of Doran & Robbers (2006), given in Eq. 3, as the standard description of EDE in the remainder of the paper. It is somewhat more closely related to the particle physics models and automatically goes to a constant energy density contribution Ω_e at early times in both the matter and radiation eras.

We compare the simulation results for this EDE model with the predictions of the Jenkins-Warren formulas in Figs. 4 and 5. Note that we do not plot the Sheth-Tormen predictions for the mass function, since we find that using the linear collapse parameter derivation from Bartelmann, Doran & Wetterich (2006) with the parametrisation of Doran (2005) leads to a limit that does not converge [2] and hence we cannot determine an appropriate δ_c. In any

---

[2] If one assumes that the overdensity of a spherical perturbation, $\Delta - 1$, is proportional to a (as in Bartelmann, Doran & Wetterich
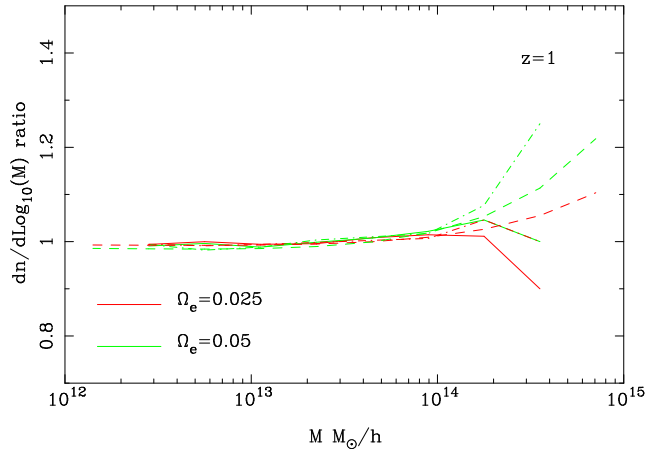
Figure 4. Mass function ratios relative to ΛCDM at $z = 1$ for two EDE models of the form in Eq. 3 with different values of Ω_e but with the cosmology fixed otherwise. The dashed lines show the Jenkins-Warren mass function prediction for the ratios while the solid lines show the simulation results using the FOF method and the dot-dashed line the results using the SO method.
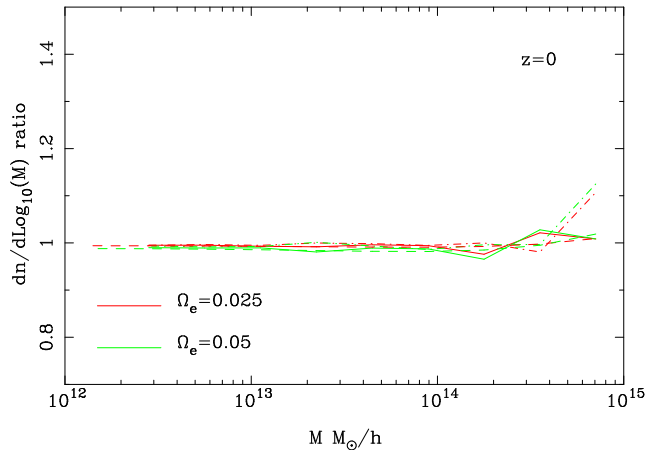

Figure 5. Mass function ratios at $z = 0$. The line styles are the same as Fig. 4.

case, the results of the previous section indicated that this approach was not suitable for EDE cosmologies.

As in Section 3.1 there are two key points to note, the first is that the difference between ΛCDM and EDE is negligible at $z = 0$ and at $z = 1$ (see Figs. 4 and 5), and second that the Jenkins-Warren mass functions correctly predict this result. Choosing to define the halos via the FOF or the SO method makes little difference to the ratio results.

The simulations used in this study are insufficient to make a precision determination of the accuracy of the Jenkins-Warren formulas for EDE cosmologies, however it is clear that they are at least accurate to $\lesssim 10\%$ for predicting the *relative* mass function of EDE and ΛCDM and future work on EDE should use these rather than the linear theory collapse motivated mass functions. If required in the future,

(2006)), then since in the Doran-Robbers model $D_+(a) \sim a^{1-(3\Omega_e)/5}$, then their ratio in Eq. 5 becomes $a^{(3\Omega_e/5)}$ and so δ_c formally goes to zero in the limit. To calculate the collapse parameter one actually needs the full numerical calculation.

larger simulations with a greater mass resolution could be used to determine the mass function for EDE cosmologies at percent level accuracy, however this is outside of the scope of this work, and unnecessary at this stage due to the lack of precision in the corresponding observations.

4 POWER SPECTRUM

The mass power spectrum is central to extracting cosmological information from galaxy redshift and weak lensing surveys. An important question is how does the addition of EDE change the non-linear mass power spectrum? Ideally we would like to be able, through simulations, to derive an understanding of the changes that EDE makes to the power spectrum, in order that we can predict this statistic for any EDE model without needing further lengthy simulations. The section presents the results of a systematic variation of cosmological parameters, in order to understand the non-linear power spectrum in EDE cosmologies.

The approach we take is to examine how the ratio of the non-linear EDE power spectrum and ΛCDM compares to *linear* power spectrum ratios. In order to turn this information into a prediction of the EDE non-linear power spectrum in general requires accurate prior knowledge of the absolute value of the non-linear power spectrum for ΛCDM, for instance the simulation calibrated, halo model motivated, formula from Smith et al. (2003) (know as Halofit), or any more accurate future method. In addition, EDE changes the shape of the linear CDM power spectrum. We therefore must calculate the correct linear power spectrum, using a package such as CMBEASY (Doran 2005), as used in this study. Armed with these two methods, we could then predict the non-linear power spectrum for EDE models *if we could relate the ratio between the EDE and ΛCDM linear and non-linear power spectra*. These will not generally be the same. This section addresses the ratio relation.

Determining the absolute value of the power spectrum is a more intensive numerical task, outside the scope of this work. However, as argued in McDonald et al. (2006) and Francis, Lewis & Linder (2007), many numerical errors will cancel in a ratio, and hence we can be confident, as long as convergence is demonstrated (see Section 2) that the ratio results are robust. Another issue is that the presence of EDE shifts the sound horizon and hence the locations in k space of the BAO peaks in the power spectrum (Doran et al. 2007; Linder & Robbers 2008). However, our simulations concentrate on the broad features of the power spectrum and do not have sufficient volume or statistics to resolve the percent level shift. Furthermore, the problem of how subtle non-linear effects alter the BAO peaks in general is an ongoing area of research (see for instance Angulo et al. (2008)). The focus of our current analysis is on the comparison between cosmologies of the broad features and small scales.

A simple first step in predicting the non-linear power in EDE cosmologies might be to use the Halofit formula with the EDE linear power and growth factor. In the subsequent sections, we present the predictions of this modified Halofit form along with our simulation results to see how useful such an approach may be. In order to make this calculation the effective spectral index n_{eff} and curvature C
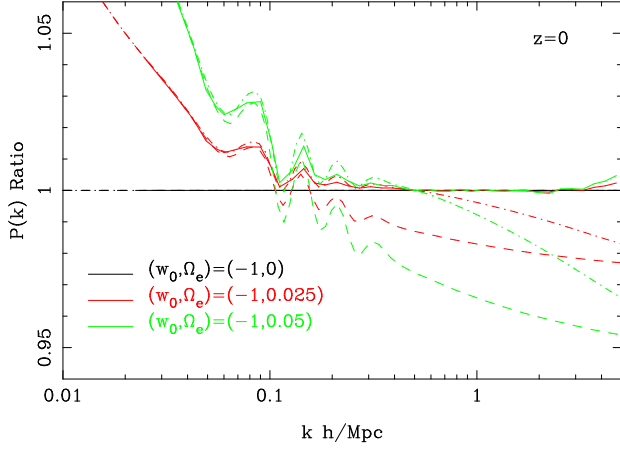
Figure 6. Keeping σ_8 constant while adding early dark energy results in a remarkably similar non-linear power for $k \gtrsim 0.2\,h/\mathrm{Mpc}$. This is despite the ratios in the linear power spectra, shown in the dashed lines, diverging. The modified Halofit prediction is shown by the dot-dashed lines.
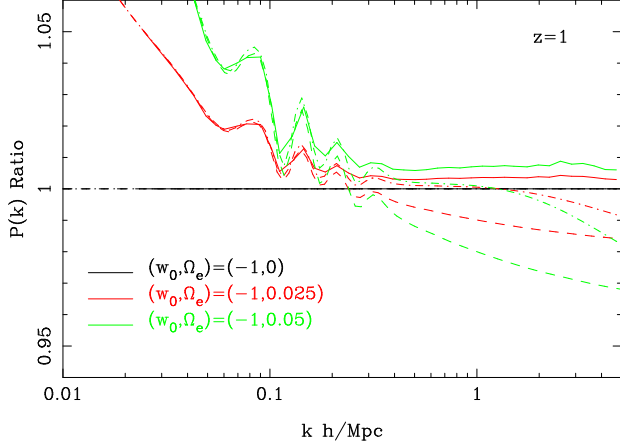

Figure 7. At $z = 1$ models with early dark energy have slightly increased non-linear power on small scales, however the shape of the relative non linear power curve differs from the linear power.

were determined from the EDE linear power spectrum. See Smith et al. (2003) for details and the Halofit formula.

4.1   Varying Ω_e

We start with a standard concordance flat ΛCDM model with parameters as given in Section 2. We then consider two EDE models with different amounts of dark energy in the early universe, Ω_e, while keeping the rest of the cosmology, including the growth normalisation today, σ_8, unaltered. The linear and non-linear mass power spectrum ratios at $z = 0$ and $z = 1$ are shown in Fig. 6 and 7.

As discussed in Section 2, the numerical convergence of the power spectrum ratios has been established at the $\sim 1\%$ level. The dependence of the ratio on numerical factors (primarily box size and particle resolution) is generally greater at higher k values. The results past $k \gtrsim 3\,h/\mathrm{Mpc}$ should perhaps be treated with more caution, but at lower k values the simulations are well converged.

Compared to ΛCDM, for a fixed primordial spectral

index n, the presence of dark energy in the early universe changes the higher k slope of the post recombination linear power spectrum, resulting in more large scale, but less small scale, linear power for the same overall normalisation σ_8. The growth amplitude in the early universe must be higher in EDE models than ΛCDM to compensate for the lower growth rate, in order to get the same σ_8 today. The relative non-linear power between EDE and ΛCDM will therefore depend on those two governing effects, i.e. the change in the linear growth rate history and the change in the initial linear power spectrum shape. Non-linear power on small scales is coupled to the power on large scales and this non-linear amplification will be enhanced in the EDE models relative to ΛCDM due to the greater amplitude of large scale power (see Figs. 6 and 7). The Halofit formula prediction (dot-dashed line in Figs. 6 and 7) should be expected to take into account at least some of the non-linear amplification effects for the EDE linear power spectrum, since this formula was calibrated based on a variety of spectral shapes. While the correct linear growth factor at any given redshift can be calculated for EDE and used in the Halofit formula for the power spectrum at that redshift, the modified growth *history* of EDE models relative to ΛCDM, will not be taken into account. Francis, Lewis & Linder (2007) and Ma (2007) found that the linear growth history in the early universe is an important factor in determining the non-linear growth at later epochs where the linear growth are matched. Therefore the scales where Halofit breaks down should grant an insight into the relative importance of the two factors, non-linear amplification and the linear growth history, as a function of scale.

The results show that the prediction of the modified Halofit formula reproduces the simulation results in the translinear regime, around $k = 0.3 - 1\,h/\mathrm{Mpc}$. As expected, the greater amplitude of large scale power in the EDE models leads to enhanced non-linear amplification and hence the non-linear power ratio is greater than the linear. Beyond $k \gtrsim 1\,h/\mathrm{Mpc}$, Halofit under-predicts the non-linear power, with the difference between this and simulations increasing with k. This can be understood from the ratio in linear growth history of the models shown in Fig. 8. The smallest scales are remembering the conditions of expansion, and linear growth, of earlier epochs, leading to a greater relative amount of non-linear growth at those scales.

In order to decouple the effects of the modified growth history and spectral shape, we performed simulations simulations in which the EDE models used the ΛCDM initial power spectrum while maintaining their correct expansion history. The $z = 0$ result for these simulations are shown in Fig. 9. In this case Halofit predicts no difference between the models, due to the common linear power spectrum shape and normalisation. Examining Figs. 6 and 9 it can be seen that the difference between the simulations and Halofit predictions in both figures are comparable. This reinforces the idea that Halofit correctly predicts much of the effects of the EDE spectral shape on intermediate scales and the modified growth history increases the power at small scales.

This comparison is not perfect and we should not expect to be able to completely decompose the effects of spectral shape and linear growth history into a linear sum. These results compare to those of Stabenau & Jain (2006) (see their Fig. 8) for the effects of a modified gravitational potential on
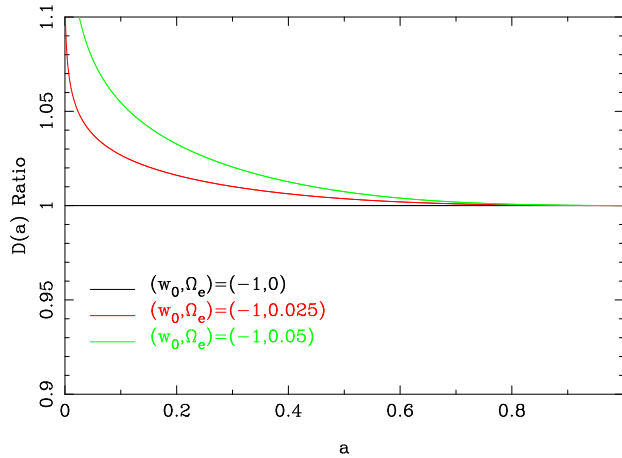
Figure 8. The linear growth factors $D(a)/D(1)$ of models with early dark energy relative to ΛCDM. The linear evolution of the growth is identical to within 1% after $z \simeq 1$.
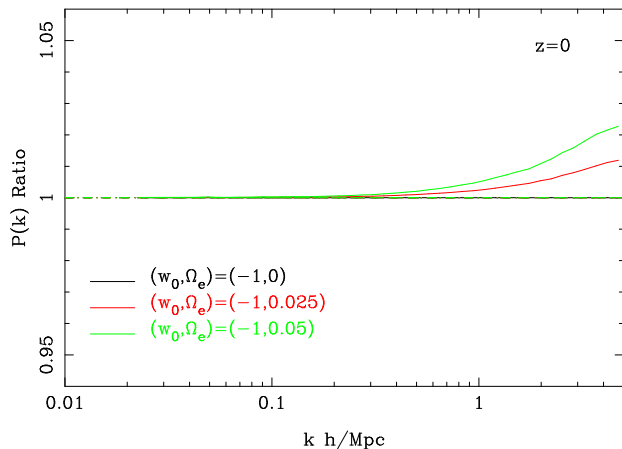

Figure 9. The same background cosmologies as Fig. 6 but using the ΛCDM initial power spectrum for all models. The higher amplitude of growth in the early universe in the EDE models leads to a greater non-linear power at small scales today.

the non-linear power spectrum. In that case, the effects on the non-linear growth of modifying the gravitational potential were found to be negligible compared with the altered linear power spectrum shape.

Note however that this is essentially the expectation previously proposed from analytic predictions of the halo mass function. The higher amplitude of growth in the early Universe in EDE models was expected to produce more collapsed structures at high redshift, with a residual increase in collapsed structures at low redshift due to the greater formation rate in the early Universe. Our power spectrum results do indicate an enhanced amount of non-linear growth relative to linear growth for the EDE models, however this enhancement is at the percent level rather than the considerable increase that would be seen if the relative halo abundance were an order of magnitude at high redshift as previously predicted.

Interestingly, the differences in the non-linear growth rates due to the spectral shape and linear growth history appear to conspire to wash out the early dark energy signal at $z = 0$. That is to say, the non-linear power in the

EDE and ΛCDM models is matched to within a percent for scales smaller than $k > 0.2\,h/\text{Mpc}$. Even at $z = 1$ (Fig. 7) the high k power in the EDE models is well matched, to about $(\Omega_e/0.05)\%$. Since we expect $\Omega_e \lesssim 0.03$ from current observational constraints, this is a remarkable match. This result accords with the mass function results of Section 3.2 that found essentially indistinguishable abundances of dark matter halos. Note that we are holding the cosmology apart from Ω_e fixed between EDE and ΛCDM. More generally we would not expect this match. For instance, a steep primordial spectral index n in an EDE model would compensate for the later flattening of the linear power spectrum due to the presence of EDE leading to a linear power spectrum after recombination much more similar to ΛCDM. In this case, as shown in Fig. 9, we would expect a greater amount of non-linear power in the EDE model.

4.2 Varying the Linear Growth History

We now examine in more detail the influence of the linear growth at different epochs on the non-linear power. In bottom-up hierarchical growth, the smallest scales reach the non-linear growth rate earlier than larger scales. We therefore expect a relationship between the relative non-linear growth at different scales imprinted on the low redshift power spectrum and the alteration of the growth rate at high redshifts. This relationship was found to be important for scales with $k \gtrsim 1\,h/\text{Mpc}$ in Section 4.1. To investigate this further, we have employed the extended EDE parametrisation suggested in the appendix of Doran & Robbers (2006)

$$\Omega_d(a) = \frac{\Omega_d^0 - \Omega_e(1 - a^{-3w_0})^\gamma}{\Omega_d^0 + \Omega_m^0 a^{3w_0}} + \Omega_e(1 - a^{-3w_0})^\gamma \quad (6)$$

where γ controls the importance of the early dark energy terms at late times. Increasing γ pushes to higher redshifts the epoch when this model changes from dark energy with a with nearly constant equation of state $w = w_0$ (i.e. ΛCDM when $w_0 = -1$) to one with appreciable early dark energy density (or w approaching 0). This extended parametrisation reduces to Eq. 3 when $\gamma = 1$. In Doran & Robbers (2006) it was found that including the extra parameter does not alter the constraints on the other cosmological parameters when fitted to the data and hence this additional parameter was not deemed necessary. However, this parameter is useful in the current study as an aid to understanding the dependence of the relative non-linear growth as a function of the high redshift linear growth behaviour. The effect of varying the γ parameter on the linear growth factor is shown in Fig. 10

How does this altered linear growth behaviour change the non-linear growth? The models shown in Fig. 10 were simulated, with the measured non-linear power spectrum results shown in Figs. 11 and 12.

At $z = 0$ (Fig. 12), models with a higher γ parameter have less non-linear power at small scales than the model with $\gamma = 1$. This can be understood from the relative linear growth histories of these models shown in Fig. 10. Since the high γ models remain more like the fiducial $w = -1$ to higher redshift, the accumulated non-linear effects due to the linear growth history are smaller in this case than for $\gamma = 1$. This causes the non-linear power to more closely track the Halofit prediction.
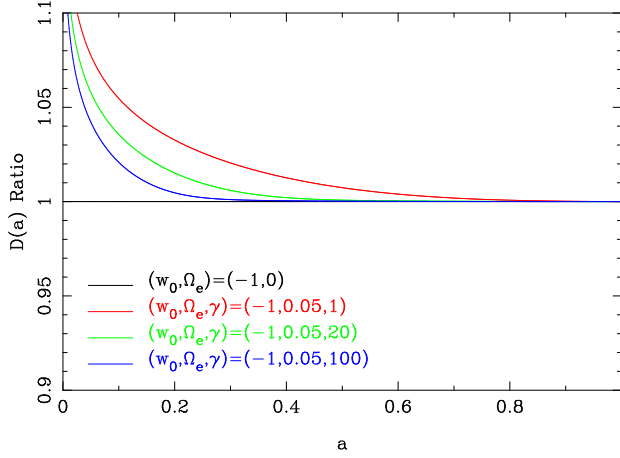
Figure 10. The effect of varying the γ parameter in Eq. 6 on the linear growth factor. Increasing the value shifts the departure from the fiducial ΛCDM to higher redshifts.
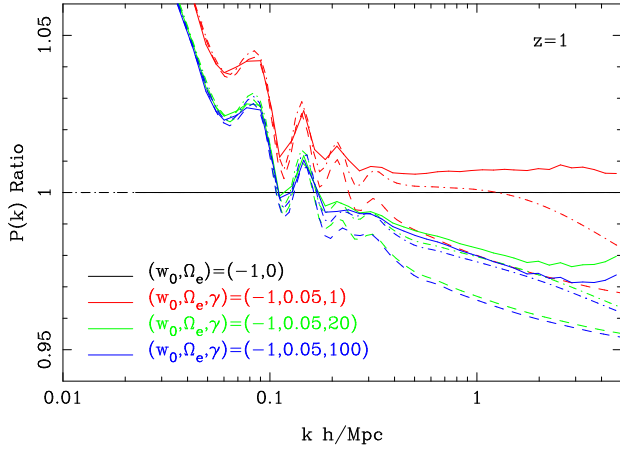

Figure 11. Power spectrum ratios with a varying γ factor at $z = 1$. The solid lines show the non-linear power while the dashed lines show the linear power, both as a ratio to the ΛCDM model.
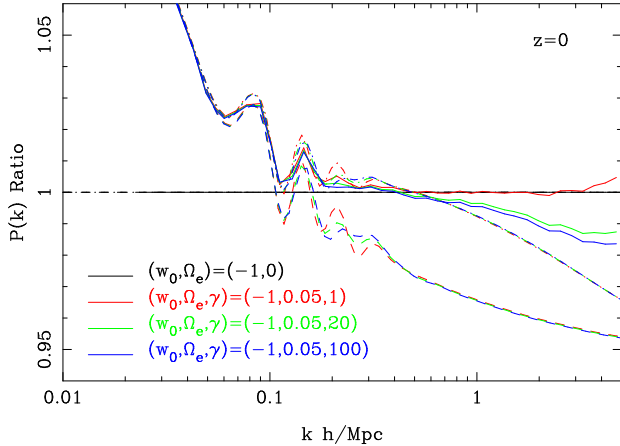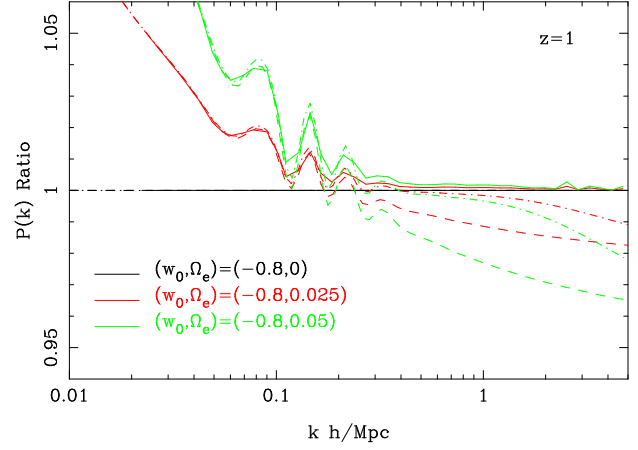

Figure 12. Power spectrum ratios with a varying γ factor at $z = 0$. The solid lines show the non-linear power while the dashed lines show the linear power, both as a ratio to the ΛCDM model.

Figure 13. Power spectrum ratios relative to a fiducial $w_0 = -0.8$ constant equation of state model. The solid lines show the non-linear power while the dashed lines show the linear power. Compared to Fig. 7, there is less difference between the linear and non-linear power spectrum ratios.

At $z = 1$ (Fig. 11) Halofit matches the simulation results well for the high γ models. Note that for both high γ models, the linear growth factor evolution is essentially identical to ΛCDM in the period between $z = 1$ and $z = 0$ (see Fig. 10). Despite this, the non-linear ratio of these models to ΛCDM does change between these two epochs. This increase is therefore due to the extra large scale power in the EDE models, and is predicted by Halofit.

Altering the linear growth history through the γ parameter demonstrates the relationship between the high redshift linear growth history and the low redshift small scale power. As found in Section 4.1, this relationship, while important, is not strong enough to cause a significant increase in small scale power in EDE models. The small scale power at low and intermediate redshift is sensitive to the high redshift linear growth history at only the percent level.

4.3 Varying the Equation of State

Until now we have compared EDE models to ΛCDM only. We will now investigate the effects from a different fiducial dark energy equation of state today, w_0. We ran a series of models with $w_0 = -0.8$, with the rest of the cosmology the same as the ΛCDM model from Section 4.1. The relative power results showed very little dependence on w_0, with the $z = 0$ results almost indistinguishable from those with $w_0 = -1$. At higher redshifts there is a weak dependence on w_0 in the non-linear power ratio, as seen by comparing the high k plateaus of Fig. 13 for $w_0 = -0.8$ vs. Fig. 7 for $w_0 = -1$.

In Fig. 13, the ratios of the linear and non-linear power spectra are more similar than in Fig. 7 where $w_0 = -1$. This can be understood from the linear growth history which, compared to Fig. 8, shows a reduced difference in the linear growth history of the models at high redshift. This is simply due to the $w_0 = -0.8$ case dark energy acting more like matter in general (due to the less negative equation of state) hence the addition of the EDE component has less influence than in the ΛCDM case.
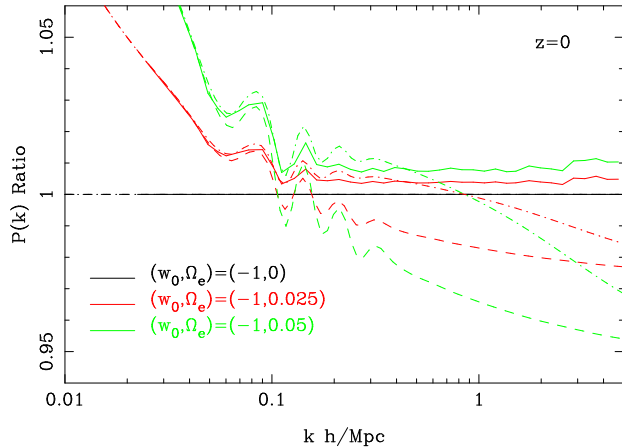
Figure 14. Power spectrum ratios relative to ΛCDM with a higher σ_8, 0.96, than that for Fig. 6 with $\sigma_8 = 0.76$. With a greater amplitude of growth, non-linear effects are enhanced and the non-linear power spectrum ratios diverge more from the linear ratios.

4.4 Varying the Growth Amplitude

The overall amplitude of structure is a major factor determining the rate of non-linear growth. It is therefore important to understand how sensitive the relative non-linear growth is to this. We have performed a series of simulations varying the linear theory σ_8 defined at $z = 0$. The result for $\sigma_8 = 0.96$ (remembering the original model shown in Fig. 6 had $\sigma_8 = 0.76$) at $z = 0$ is shown in Fig. 14. As might be expected, while σ_8 scales out in the linear power ratios (so the dashed lines are the same as in Fig. 6), the higher amplitude of growth leads to enhanced non-linear effects. The difference in the non-linear and linear power spectrum ratios is increased with increasing σ_8. The results for $z = 1$ have a similar increase in the power spectrum ratio and are not shown for brevity.

Once again we can see that the modified Halofit formula matches the simulation results well at intermediate scales but under predicts the power in the EDE models on smaller scales. The scale where Halofit begins to under predict the EDE power is pushed to a lower k value, again due to the increased non-linear effects from the higher growth amplitude normalisation.

To test our intuition about effects governing the power spectrum results, we also ran simulations with fixed primordial power spectrum amplitude A_s rather than σ_8. The $z = 0$ result is shown in Fig. 15. For these simulations, one gets different linear power today (and so different σ_8) but the early epochs of collapse, showing up in the very nonlinear (higher k) regime today, are more similar. This can be seen in the power for $k > 1 \, h/\text{Mpc}$ in the EDE models which increases with k, heading back towards the ΛCDM power since the amplitude of power in the different models was more similar when those scales collapsed than it is today.

Matching σ_8 appears to be sufficient to ensure that the small scale non-linear power between ΛCDM and EDE models are matched to within a few percent, regardless of the amount of early dark energy, Ω_e (see Fig. 6) or the redshift when this EDE term turns on (see Fig. 12). This match is weakly dependent on σ_8; however varying σ_8 by 0.2, a considerable amount, shifts the ratio in power by only a percent.
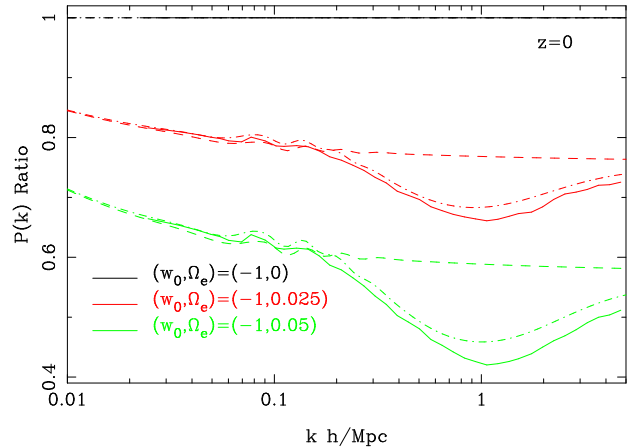

Figure 15. Simulations with fixed primordial amplitude A_s rather than fixed σ_8 today.

These results leads to a useful tool for confronting EDE models with power spectrum measurements, such as galaxy redshift surveys or weak lensing. The Halofit formula, modified by using the EDE linear power spectrum and growth factor, predicts the non-linear power ratio to within a percent out to $k \sim 1 \, h/\text{Mpc}$. For smaller scales, using the ΛCDM non-linear power matches the EDE result to within a few percent or so, particularly at low and zero redshift. This prescription is fairly loose but could be improved upon with a more quantitative study of the variation in power with cosmological parameters. The main point from this study is that the variations between EDE and ΛCDM are at the few percent level only, rather than there being a significant difference in non-linear power.

4.5 Growth vs. Geometry

The expansion history of an EDE model can be fit well out to $z = 2$ with a time varying equation of state $w(a) = w_0 + w_a(1 - a)$ with $w_a \approx 5\Omega_e$. Fig. 16 shows the dark energy density and equation of state for an EDE model and the matching (w_0, w_a) model. Distance measurements, such as from Type Ia supernovae, will agree in the two models to 0.02% out to $z = 2$. However, the early universe histories were very different. Does the growth history distinguish between these two models? To investigate this question, we simulated a pair of models, one using the Eq. 3 form of EDE with $\Omega_e = 0.03$ and $w_0 = -0.95$ and one using the (w_0, w_a) form of dark energy with $w_0 = -0.95$ and $w_a = 0.15$ with the cosmology matched otherwise. The power spectrum ratio results are shown in Figs. 17 and 18.

In this case the EDE model is taken as the fiducial, and we display the ratio of the (w_0, w_a) model to this. Once again, we see that the non-linear power on small scales is well matched between the two models, despite the linear power ratios not matching at these scales. At $z = 1$ the difference between the linear and non-linear ratios is less, with more non-linear power at small scales in the (w_0, w_a) model. Once again it is instructive to examine the linear growth history, shown in Fig. 19.

This figure shows that the EDE model has a higher amplitude of growth in the early universe than the (w_0, w_a) model. This is due to the greater amount of dark energy
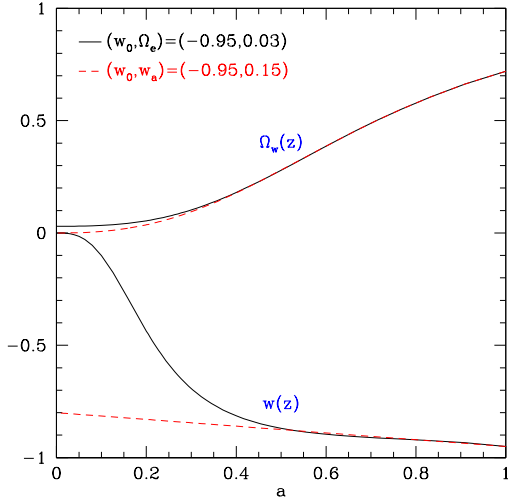
Figure 16. Dark energy density and equation of state comparison for an EDE and (w_0, w_a) model with distance history matched to 0.02% out to $z = 2$.
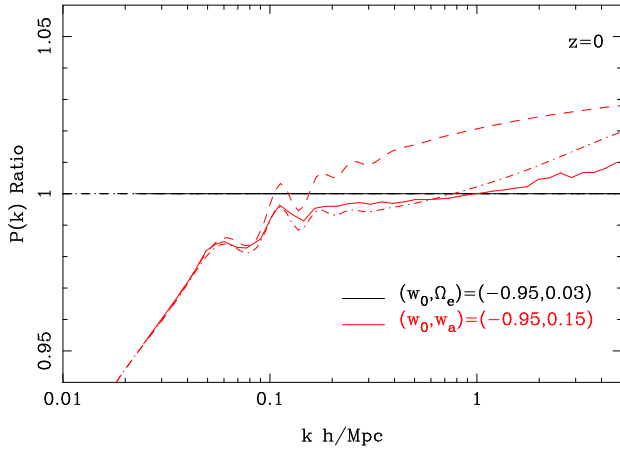

Figure 17. Ratio results at $z = 0$ for the comparison between the two parameterisations for dark energy given by $w(a) = w_0 + w_a(1-a)$ and Eq. 3, where the parameter values are chosen match to the distance history.
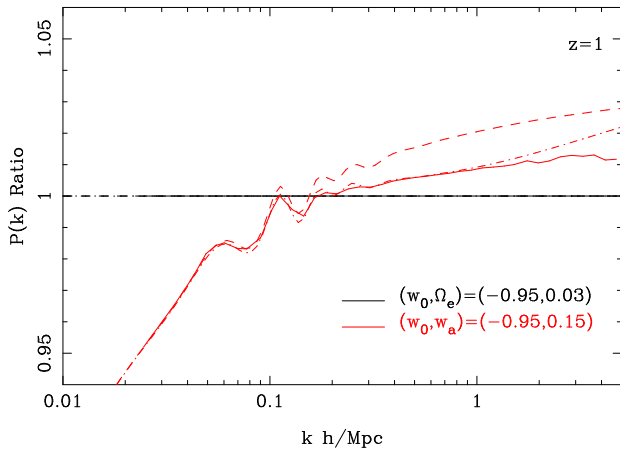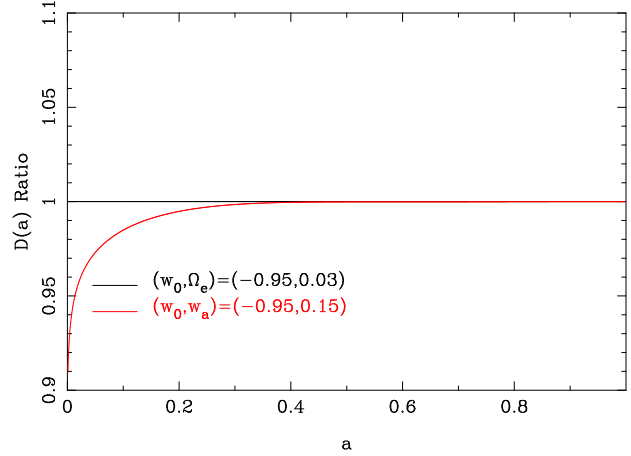

Figure 18. As Fig. 17 but at $z = 1$.

Figure 19. The relative linear growth factor evolution for the EDE and (w_0, w_a) models with matching distance history.

present at this time, leading to less linear growth over the whole history of the universe, requiring the EDE model to start at a higher growth amplitude in order to obtain the same linear theory σ_8 today. The linear growth factor is very well matched between the two models after $z \approx 2$ ($a \approx 0.33$), yet as can be seen, the non-linear growth between $z = 1$ and $z = 0$ is different in the two models, again due to the nonlinearity amplification effect.

5   CONCLUSIONS

In this work we have examined the effects of early dark energy on the non-linear growth of structure through N-body simulations. The key result is that non-linear large scale structure, including the abundance of clusters, is relatively insensitive to the presence of EDE. This result is in contrast to previous analytic work which expected a substantial increase in non-linear structure compared to ΛCDM with the same σ_8.

The implications of the results presented here are that EDE is much more difficult to detect than previously thought. This presents a problem for dark energy cosmology, not only for the sake of understanding dark energy but because, as shown in Doran et al. (2007) and Linder & Robbers (2008), the presence of EDE can significantly bias distance measurements using baryon acoustic oscillations if the possibility of EDE is not considered. Fitting for EDE however significantly reduces the discriminating power of BAOs.

Ideally it was hoped to detect the presence of EDE through cluster abundances (see Fedeli & Bartelmann (2007)), such as with future Sunyaev-Zel'dovich, weak lensing, X-ray, or optical surveys. This would provide an independent measure of EDE thus restoring the discriminating power of BAO measurements. However, this work demonstrates that this is not the case.

As the amount of EDE increases, it becomes easier to distinguish in that the primordial amplitude of matter density perturbations must be increased to reach the same growth (σ_8) by today. Such effects in linear growth and the CMB anisotropy power spectra allow that EDE must contribute less than a few percent to the early energy

density (Doran, Robbers & Wetterich 2007). The acoustic sound horizon shifts by approximately half of this. However this article shows that observations of non-linear structure should not be expected to provide a substantial leap in our ability to detect EDE.

This study has demonstrated that the halo mass function formulas of both Jenkins et al. (2001) and Warren et al. (2006) are valid for predicting the EDE to ΛCDM results ratio to within $\sim 10\%$ or better in the mass range $\sim 10^{12} - 10^{15} M_\odot$. Future studies of EDE should use these formulas or N-body simulations when considering halo abundances, rather than spherical collapse motivated mass functions as have been used in the past.

We have also demonstrated that the Halofit (Smith et al. 2003) formula for the non-linear power spectrum, when using the EDE linear matter power spectrum and growth factor, is accurate for EDE cosmologies for scales larger than around $k \sim 1\,h/\mathrm{Mpc}$. On smaller scales this formula under predicts the power. Further work would be needed to accurately re-calibrate this formula for EDE on these scales, perhaps along the lines of the way McDonald et al. (2006) corrected Halofit for constant w dark energy cosmologies. Until such a study is performed we propose, as discussed in Section 4.4, that the results of this study suggest a simple prescription for predicting the non-linear power spectrum for EDE models to within an accuracy of a percent or so relative to the ΛCDM prediction.

ACKNOWLEDGMENTS

REFERENCES

Angulo, R. E., Baugh, C. M., Frenk, C. S., & Lacey, C. G. 2008, MNRAS, 383, 755

Bartelmann, M., Doran, M., & Wetterich, C. 2006, A&A, 454, 27

Copeland, E., Sami, M. & Tsujikawa, S. Int.J.Mod.Phys. D15 (2006) 1753-1936

Davis, M., Efstathiou, G., Frenk, C. S., & White, S. D. M. 1985, ApJ, 292, 371

Doran, M. 2005, Journal of Cosmology and Astroparticle Physics, 10, 11

Doran, M., Schwindt, J.-M., & Wetterich, C. 2001, PhRvD, 64, 123520

Doran, M., & Robbers, G. 2006, Journal of Cosmology and Astroparticle Physics, 6, 26

Doran, M., Robbers, G., & Wetterich, C. 2007, PhRvD, 75, 023003

Doran, M., Stern, S., & Thommes, E. 2007, Journal of Cosmology and Astroparticle Physics, 4, 15

Fedeli, C., & Bartelmann, M. 2007, A&A, 461, 49

Francis, M. J., Lewis, G. F., & Linder, E. V. 2007, MNRAS, 380, 1079

Gill, S. P. D., Knebe, A., & Gibson, B. K. 2004, MNRAS, 351, 399

Jenkins, A., Frenk, C. S., White, S. D. M., Colberg, J. M., Cole, S., Evrard, A. E., Couchman, H. M. P., & Yoshida, N. 2001, MNRAS, 321, 372

Komatsu, E., et al. 2008, ArXiv e-prints, 803, arXiv:0803.0547

Kowalski, M., et al. 2008, ArXiv e-prints, 804, arXiv:0804.4142 (accepted by ApJ

Linder, E. V. 2006, Astroparticle Physics, 26, 16

Linder, E. V., & Jenkins, A. 2003, MNRAS, 346, 573

Linder, E. V., & Robbers, G. 2008, Journal of Cosmology and Astroparticle Physics, 6, 4

Lukić, Z., Reed, D., Habib, S., & Heitmann, K. 2008, ArXiv e-prints, 803, arXiv:0803.3624

Ma, Z. 2007, ApJ, 665, 887

Ma C. & Bertschinger E., 1995, ApJ, 455, 7

McDonald, P., Trac, H., & Contaldi, C. 2006, MNRAS, 366, 547

Perlmutter, S., et al. 1999, ApJ, 517, 565

Power, C., & Knebe, A. 2006, MNRAS, 370, 691

Press, W. H., & Schechter, P. 1974, ApJ, 187, 425

Riess, A. G., et al. 1998, AJ, 116, 1009

Sadeh, S., Rephaeli, Y., & Silk, J. 2007, MNRAS, 380, 637

Sadeh, S., & Rephaeli, Y. 2008, MNRAS, 388, 1759

Sheth, R. K., & Tormen, G. 1999, MNRAS, 308, 119

Smith, R. E., et al. 2003, MNRAS, 341, 1311

Springel V., 2005, MNRAS, 364, 110

Stabenau, H. F., & Jain, B. 2006, PhRvD, 74, 084007

Waizmann, J.-C., & Bartelmann, M. 2008, ArXiv e-prints, 804, arXiv:0804.2815

Warren, M. S., Abazajian, K., Holz, D. E., & Teodoro, L. 2006, ApJ, 646, 881

Wetterich, C. 1988, Nucl. Phys. B 302, 668

Wetterich, C. 2004, Physics Letters B, 594, 17

Zel'dovich, Y. B. 1970, A&A, 5, 84

This paper has been typeset from a TEX/ LATEX file prepared by the author.